

**COMPUTER-AIDED DESIGN OF 30 KW HORIZONTAL AXIS WIND TURBINE BLADES****Davor JOVANOVIC<sup>1,\*</sup> - Vanja SUSTERSIC<sup>1</sup>**<sup>1</sup> University of Kragujevac, Faculty of Engineering, Kragujevac, Serbia**Received** (05.09.2019); **Revised** (09.12.2019); **Accepted** (11.12.2019)

**Abstract:** Blade geometry optimization for 30 kW wind turbine with 6.5 tip speed ratio is applied via Betz and Schmitz formulas, using “QBlade” software. These formulas were applied to modify chord distribution and twist angle of airfoil SD7062. Using the same software, 3D model of blades and rotors for both cases are generated. Afterwards, BEM simulation is conducted in the “QBlade” for both cases and values of power coefficient depending on tip speed ratio, as well as power output depending on wind speed for both optimised wind turbines is obtained. These values for both cases are used to determine annual energy production, while using Weibull distribution to determine probability for certain wind speeds to occur. Shape (*k*) and scale (*c*) parameters were identical in both simulations. After conducted simulations, it is noted that Betz optimised rotor has higher peak for power production, compared to the Schmitz optimised rotor. Also, both rotors have slightly different power coefficients depending on tip speed ratio. Using Weibull equations, it is estimated that Betz optimised rotor has 2.79% higher annual energy production, compared to the Schmitz optimised rotor.

**Key words:** Betz, BEM, Schmitz, Weibull distribution, Annual energy production**1. INTRODUCTION**

Constant population growth leads to increased energy consumption, therefore, there is growing necessity for energy source that cannot be depleted (coal, oil, natural gas, etc.) before its regeneration. According to [1] preliminary data, by the end of 2018 there is around 600 GW of wind turbine installed capacity, which presents near 10% of growth in energy production, compared to 2017, when there was around 546 GW of installed wind turbine capacities. According to [2] it is estimated that global wind turbine market will reach \$47.86 billion in 2022. According to [3], installed wind capacity in R. Serbia ranges from 10 MW to 25 MW throughout years 2015 to 2017, respectively. These data show that Serbia is in steady increase of wind energy production capacity.

Software “QBlade” is an open source program, which generates and optimizes 3D geometry of rotors based on input parameters, which is convenient for preliminary analysis and is relatively simple to use (compared to other software like CFD, SOLIDWORKS, FlowVision, etc., where preliminary analysis can be quite complicated). Many researches were conducted using simple Blade Element Momentum (BEM) theory for horizontal three-bladed wind turbines. In [4] experimental and numerical methods were used to test three different horizontal axis wind turbine blade shapes, whereas it is concluded that BEM theory is not only useful for designing the optimal blade shape, but also to predict blade performance. In [5] aerodynamic investigation using numerical simulation of 10 kW horizontal wind turbine was conducted, where it was concluded that there is a good comparison of torque and thrust between numerical simulation and improved BEM theory. In [6] a unique approach was developed using BEM method to obtain the optimal twist angle and

chord length for small wind turbine design. Also, in [7] and [8] comparison of CFD and “QBlade” results for small-scaled wind turbines is conducted for torque vs tip speed ratio (TSR) and velocities at 15 m/s, respectively. There are other computer-aided designs that were conducted for horizontal three bladed wind turbines, like [9] where blade is divided into structural and dynamic surfaces with a continuity imposed on their connecting regions, or [10] where blades were modelled using B-spline surfaces.

**2. MATERIALS AND METHODS****2.1. Chord distribution, twist angle optimization**

Basic parameters for analyzed wind turbine are following:

- Rated power: 30 kW,
- Number of blades: 3,
- Blade length: 5.8 m,
- Rotor radius: 6.25 m,
- Rated wind speed: 9.8 m/s,
- Stalled power regulation.

Chord and twist angle will be calculated according to the following Betz formulas [11-14]:

$$c(r) = \frac{16 \cdot \pi \cdot R}{9 \cdot B \cdot C_L(\alpha) \cdot \lambda} \cdot \frac{1}{[(\lambda \cdot \frac{r}{R})^2 + \frac{4}{9}]^{1/2}} \quad (1)$$

$$\beta(r) = \frac{2}{3} \cdot \tan^{-1} \left( \frac{R}{r \cdot \lambda} \right) \quad (2)$$

Where R and r are radius and local radius of the rotor, respectively (see figure 1). B stands for number of blades

\*Correspondence Author's Address: University of Kragujevac, Faculty of Engineering, Sestre Janjic 6, 34000 Kragujevac, Serbia, davorjovanovic94@gmail.com

for analysed wind turbine while  $\lambda$  stands for tip speed ratio (TSR), which is calculated based on equation (3). Lift coefficient  $C_L(\alpha)$  is determined based on chosen (calculated) foil from the foil database [15] and relative angle of attack  $\alpha$  which value fits minimum value of  $C_L/C_D$  ratio. Where  $C_D$  stands for drag coefficient. This is due to BEM analysis assumption that  $C_D = 0$ . Therefore, from figure 3  $\alpha$  will be determined from maximum  $C_L/C_D$  ratio and afterwards value for  $C_L$  (for determined angle) from figure 4, which will be used in calculations [12-14].

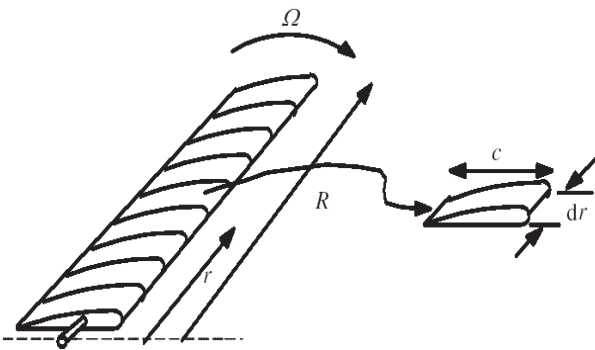


Fig.1. Schematic representation of blade elements, where  $\Omega$  stands for angular velocity,  $c$  stands for chord and  $dr$  for radial element dimension

TSR is determined from the following equation [12], [16], [17]:

$$\lambda = \frac{R \cdot \Omega}{v} = \frac{D \cdot \pi \cdot N}{60 \cdot v} \quad (3)$$

Where D is rotor diameter in m (12.5 m),  $v$  is rated wind speed (9.8 m/s) and N is number of rotor turns per minute. Since three-bladed wind turbines have high  $C_p$  (power coefficient) within the range of TSR from 6 to 8, a value of 6.5 is chosen for the analysis. If we substitute value of 6.5 in equation (3), rotor would have 97.3 rpm, which will be used when conducting BEM analysis for wind turbine power curve [13, 14].

Blade optimization after Schmitz will also be conducted, according to the equation [11], [18]:

$$c(r) = \frac{16 \cdot \pi \cdot R}{B \cdot C_L(\alpha) \cdot \lambda} \sin^2 \left( \frac{1}{3} \cdot \tan^{-1} \left( \frac{R}{\lambda \cdot r} \right) \right) \quad (4)$$

Note that during the analysis chord length distribution for designed airfoil will be optimized, thus, twist angle will be identical for both cases (optimized to yield highest angle of attack ratio for each section after preliminary calculation, according to [13]).

## 2.2. Airfoil selection

Airfoil SD7062 will be used in this analysis, according to recommendation for small wind turbines [19]. Experimental data for lift and drag coefficients depending on the relative angle of attack are obtained from *National Advisory Committee for Aeronautics* (NACA) [15]. By examining figure 2 it can be noticed that  $C_L/C_D$  ratio has a highest value of 121.5468, which fits relative angle of attack  $\alpha = 6^\circ$ . By looking at figure 3, for determined relative angle of  $6^\circ$  fits value of 1.1158 for  $C_L$ . These

values will be used in equations (1) and (2) when determining chord distribution and twist angle for the foils.

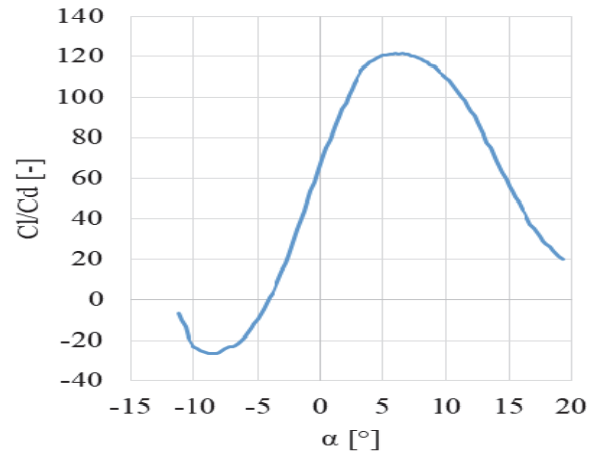


Fig.2. Values for  $C_L/C_D$  ratio depending on the relative angle  $\alpha$

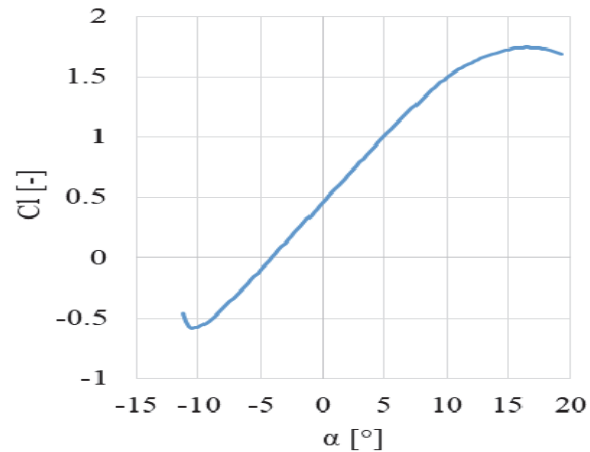


Fig.3. Values for  $C_L$  depending on the relative angle  $\alpha$

## 2.3. BEM Theory

BEM theory consists of two basic models that a blade is created from large number of elements which are infinitely small and that those elements are aerodynamically independent, thus, what happens to any element of a blade, doesn't affect the adjacent ones. This theory combines blade element theory and momentum theory, thus the thrust and torque of each element is determined, which is then added thrust and torque of other elements to define the final thrust and torque generated from a blade. Therefore, it is possible to determine power output using this theory, via following equation [12-14]:

$$C_P = \frac{8}{\lambda^2} \int_{\lambda_0}^{\lambda} Q \cdot \lambda_r^3 \cdot a' \cdot (1-a) \cdot \left[ 1 - \frac{C_D}{C_L} \tan \alpha \right] d\lambda_r \quad (5)$$

Where  $a$  and  $a'$  are axial and radial induction factors which are calculated using following equations (for angle and induction factors see figure 4), respectively, these values are calculated via iteration [12-14]:

$$\frac{a}{1-a} = \frac{\sigma' \cdot [C_L \cdot \sin \alpha + C_D \cdot \cos \alpha]}{4 \cdot Q \cdot \cos^2 \alpha} \quad (6)$$

$$\frac{a'}{1-a} = \frac{\sigma' \cdot [C_L \cdot \cos \alpha - C_D \cdot \sin \alpha]}{4 \cdot Q \cdot \lambda_r \cos^2 \alpha} \quad (7)$$

Where  $\lambda_r$  is local TSR, which is defined and calculated via equation (8), while Q represents tip loss corrections and is calculated via equation (9). Also,  $\sigma'$  is solidity of the turbine rotor and it is expressed in equation (10) [12-14], [16], [20]:

$$\lambda_r = \lambda \cdot \frac{r}{R} \quad (8)$$

$$Q = \frac{2}{\pi} \cdot \cos^{-1} \left( e^{\frac{B}{2} \cdot (1-\frac{r}{R}) \cdot (\frac{r}{R} \cdot \cos \alpha)^{-1}} \right) \quad (9)$$

$$\sigma' = \frac{B \cdot c}{2 \cdot \pi \cdot r} \quad (10)$$

Note that  $\lambda_h$  used in equation (5) stands for TSR at the hub radius, thus, local TSR at the beginning of blade root which is exposed to wind.

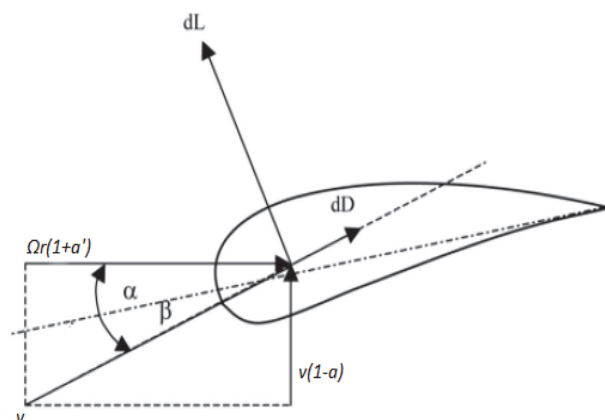


Fig.4. Schematic representation of forces acting on blade

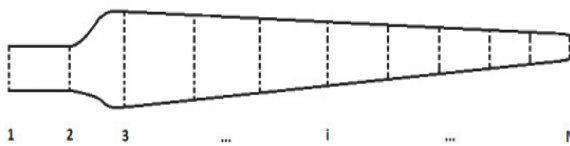


Fig.5. Foil distribution along the blade with N number sections

In order to complete the BEM simulation, it is necessary to divide blades into N elements (see figure 5), in the conducted simulations the blades are divided into 100 elements. Note that in figure 4 there are forces  $dD$  and  $dL$ , which stand for elementary drag and lift force, obtained as a result of transformed kinetic energy of the wind, respectively. Finally, the power that is generated on wind turbine is determined based on  $C_p$  definition [14]:

$$C_p = \frac{P}{P_{wind}} = \frac{P}{\frac{1}{2} \cdot \rho \cdot A \cdot v^3} \Rightarrow P = \frac{1}{2} \cdot C_p \cdot \rho \cdot A \cdot v^3 \quad (11)$$

Where  $P_{wind}$  stands for power generation without any losses, thus, ideal wind power generation,  $\rho$  stands for wind density ( $1.222 \text{ kg/m}^3$  in this analysis) and A for rotor surface.

## 2.4. Weibull Distribution

In order to determine annual energy production for each wind turbine, Weibull distribution equations are applied. According to those equations, probability for certain wind speed to occur between any given values is determined. Therefore, given the probability, annual energy production can be specified. Equation for certain wind speed to occur is [13], [16], [21]:

$$f(v) = \frac{k}{c} \cdot \left(\frac{v}{c}\right)^{k-1} \cdot e^{-\left(\frac{v}{c}\right)^k} \quad (12)$$

Where k and c are shape and scale parameter, which determine the shape and interval of wind speed where the curve stretches (see figure 6), respectively. Probability for a certain wind speed to occur between  $v_i$  and  $v_{i+1}$  is described via the following formula [13], [16], [21]:

$$f(v_i < v < v_{i+1}) = e^{-\left(\frac{v_i}{c}\right)^k} - e^{-\left(\frac{v_{i+1}}{c}\right)^k} \quad (13)$$

Taking into consideration equations (12) and (13) annual energy production can be computed via equation [13], [16], [21]:

$$AEP = \sum_{i=1}^{N-1} \frac{1}{2} \cdot (P(v_{i+1}) + P(v_i)) \cdot f(v_i < v < v_{i+1}) \cdot 8760 \quad (14)$$

Where N stands for highest number of velocities that are taken into account for determination of probability and constant 8760 stands for number of hours during one year.

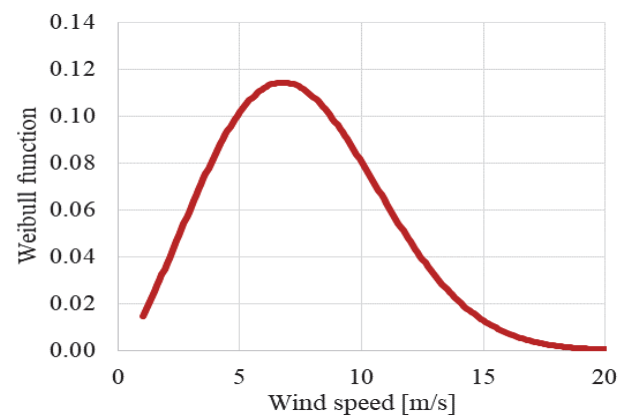


Fig.6. Weibull distribution depending on the wind speed ( $v$ ) which is the same for both cases

For the analysis value for  $k = 2.38$  and  $c = 8.5 \text{ ms}^{-1}$  will be assumed [22]. These parameters will be the same in both cases, so annual power generation difference could be precisely determined.

### 3. RESULTS AND DISCUSSION

According to defined parameters and equations in previous sections, twist angle and chord is calculated. Afterwards, optimization in “QBlade” software is conducted, whereas, the twist angle and blade chord distribution are shown in figures 7 and 8, respectively.

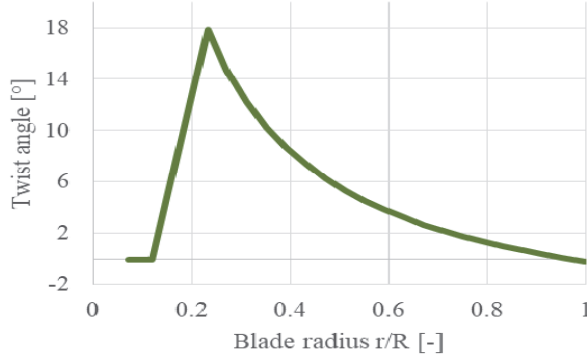


Fig.7. Twist angle distribution which is applied for Betz and Schmitz blades

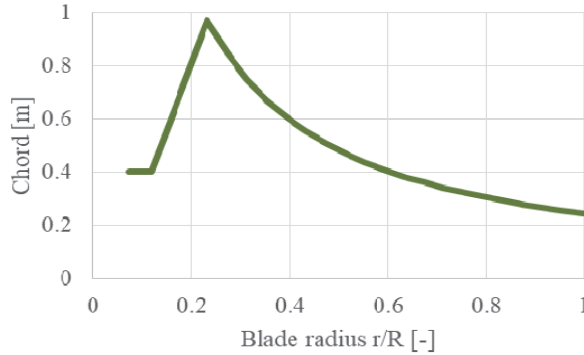


Fig.8. Chord distribution for Betz optimal blade

According to the values shown in figures 7 and 8, blade and rotor 3D model in software “QBlade” is generated, with presented local radius of each foil and hub taken into account in terms of rotor radius increase, as shown in figures 9 and 10.

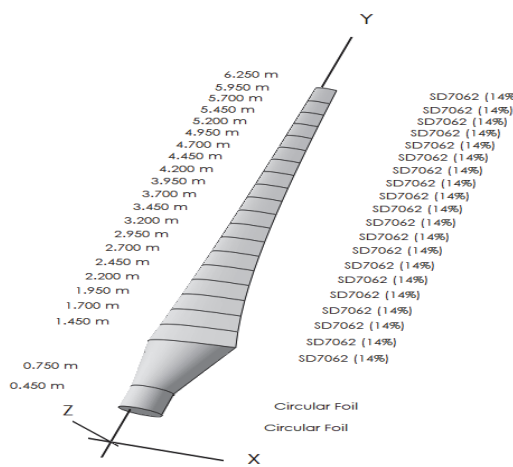


Fig.9. Generated 3D model of blade, according to Betz optimisation equations

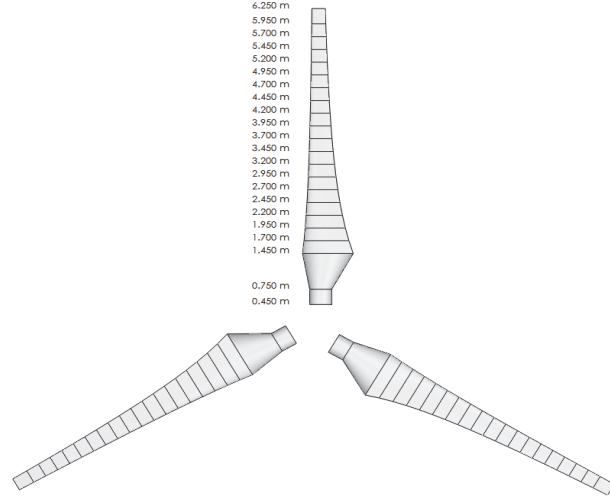


Fig.10. Generated 3D model of turbine rotor, according to Betz optimisation equations

Chord distribution and generated 3D model of blade, according to Schmitz optimization equations are shown in figures 11 and 12, respectively. Note that there is slightly different chord distribution between Betz and Schmitz blades (see figures 8 and 11), whereas, Betz maximum foil chord is 0.969 m at 1 m local radius, while Schmitz maximum foil chord is 0.816 m at the same local radius. This pattern in chord difference is followed throughout each sections of blades.

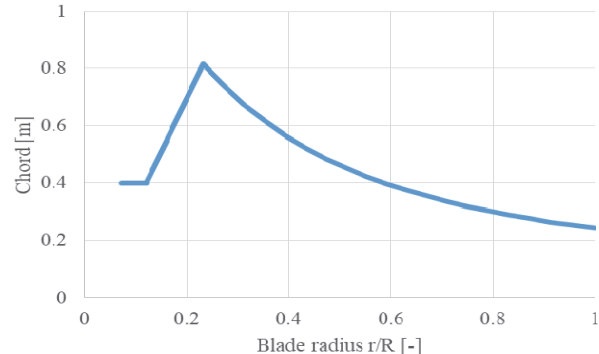


Fig.11. Chord distribution for Schmitz optimal blade

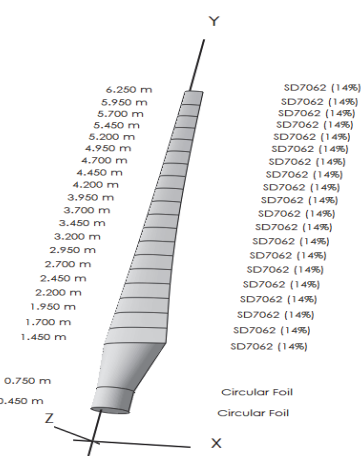


Fig.12. Blade 3D model, according to Schmitz optimisation equations

After both blades are calculated and 3D models are created, BEM analysis is conducted for both blades. In figures 13 and 14 is shown power curve for both cases, which are generated after BEM theory is applied on 100 aerodynamically independent elements. Note that cut-in wind speed is  $3 \text{ ms}^{-1}$  and cut-out is  $30 \text{ ms}^{-1}$ .

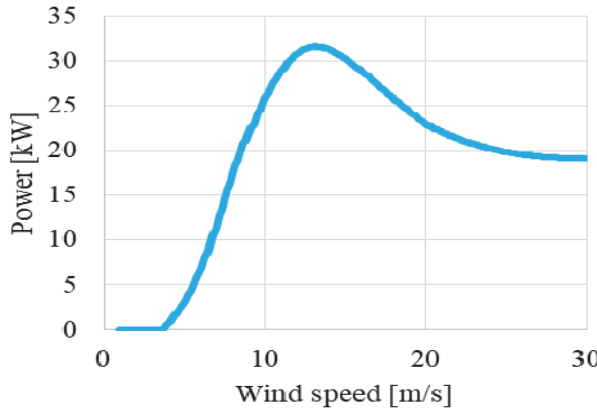


Fig.13. Power curve generated for Betz optimized rotor

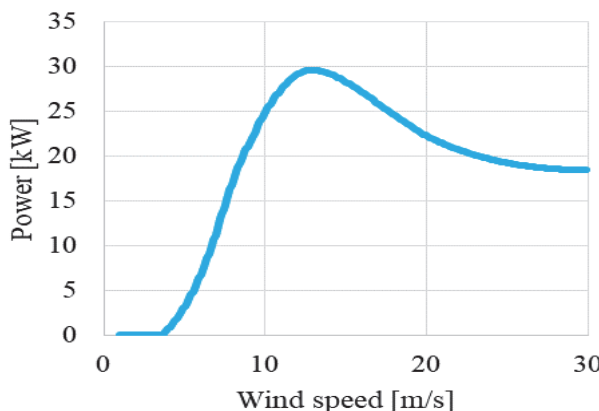


Fig.14. Power curve generated for Schmitz optimized rotor

From figures 13 and 14 can be seen a clear difference between highest power capacity for both rotors. Betz optimised rotor has a highest power generation at  $13.1 \text{ ms}^{-1}$  with 31.55 kW, while Schmitz optimized rotor has highest power generation at  $12.9 \text{ ms}^{-1}$  with 29.56 kW. This gap close to 2 kW will have some effect in annual energy production. Note that power curves for both cases are slightly different, whereas, power curve for Schmitz optimized rotor has a bit lower value for corresponding wind speeds than the Betz optimized rotor.

After conducted BEM analysis, power coefficient ( $C_p$ ) depending on TSR can be graphically presented (see figures 15 and 16). This coefficient has a direct effect at power curve for analysed rotors, according to equation (11).

By analysing figures 15 and 16, small  $C_p$  difference can be noticed. Highest  $C_p$  ratio for Betz optimised rotor is 0.458 at 5.23 TSR, while for Schmitz optimised rotor  $C_p$  ratio is 0.46 at 5.3 TSR. While these are highest values of  $C_p$  ratio, at rated TSR (6.5) according to which both rotors are calculated these values are 0.416 and 0.418 for Betz

and Schmitz optimised rotor, respectively. This difference has slight impact at power output for both wind turbines.

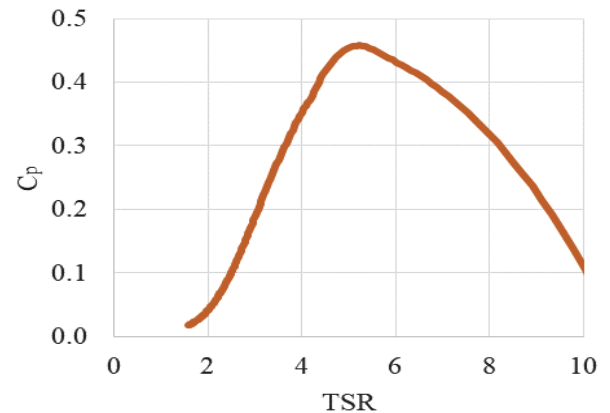


Fig.15. Power coefficient for Betz optimized rotor

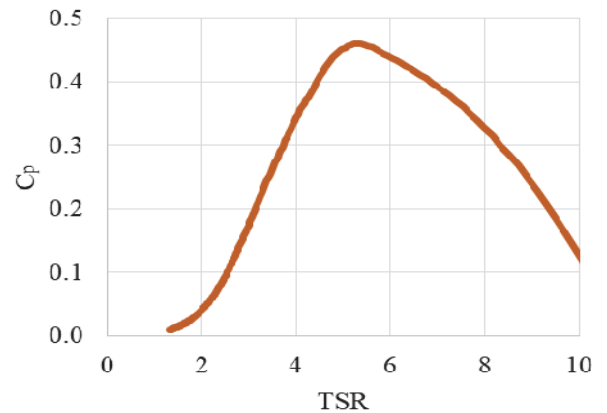


Fig.16. Power curve for Schmitz optimized rotor

By using data from figure 6, AEP from equation (14) can be determined for both rotors. Therefore, AEP for Betz optimised rotor is 124142 kWh, while for Schmitz optimised rotor AEP is 120775 kWh. Considering these two values, it can be noticed that Betz optimised rotor has 2.79% higher AEP. Therefore, for preliminary wind turbine analysis using “QBlade” software, it is recommended to use Betz blade optimisation, as it produces more annual energy than Schmitz optimised rotor for the same parameters and conditions.

#### 4. RESULTS AND DISCUSSION

By using software “QBlade”, power curve of wind turbine with rated power of 30kW, TSR of 6.5 and rated wind speed of  $9.8 \text{ ms}^{-1}$  is analysed using Betz and Schmitz formulas for blade geometry optimisation. Chord distribution is optimised, while twist angles are same for both cases when calculated and optimised so angle of attack has maximum value. 3D models of blades and rotors are generated and BEM analysis is conducted (for 100 elements blade discretization), thus, calculating power curves and power coefficients. Weibull distribution is used to calculate probability for certain wind speeds to occur (parameters  $k$  and  $c$  are the same for both cases with values of 2.38 and  $8.5 \text{ ms}^{-1}$ ). It is noted that, observing wind turbine of 30kW differences in power curves and power coefficients cause 2.79% higher energy

production annually for Betz optimised blades, compared to Schmitz optimisation.

## REFERENCES

- [1] (2018) <https://library.wwindea.org> - Wind Energy International, Global Wind Installations, Accessed on: 2019-03-17
- [2] (2017) <https://www.globaldata.com> - GlobalData, Wind Turbines, Update 2018 - Global Market Size, Competitive Landscape, Key Country Analysis to 2022, Accessed on: 2019-03-18
- [3] (2018) <http://resourceirena.irena.org> - IRENA, Final Renewable Energy Consumption, Accessed on: 2019-03-18
- [4] Hsiao, B.; Bai, J. & Chong, T. (2013). Energies. *The Performance Test of Three Different Horizontal Axis (HAWT) Blade Shapes Using Experimental and Numerical Methods*, Vol.6, No.6 (June 2013) pp. 2784-2803, 1996-1073
- [5] Bai, J.; Hsiao, B.; Li, H.; Huang, Y. & Chen, Y. (2013). Procedia Engineering. *Design of 10 kW Horizontal-Axis Wind Turbine (HAWT) Blade and Aerodynamic Investigation Using Numerical Simulation*, Vol.67, (December 2013) pp. 279-287, 1877-7058
- [6] Tang, X.; Huang, X.; Peng, R. & Liu, X. (2015). Procedia CIRP. *A Direct Approach of Design Optimization for Small Horizontal Axis Wind Turbine Blades*, Vol.36, (December 2015) pp. 12-16, 2212-8271
- [7] Koc, E.; Günel, O. & Yavuz, T. (2016). Comparison of Qblade and CFD results for small-scaled horizontal axis wind turbine analysis, Switzerland, Available from: [https://www.researchgate.net/publication/315854164\\_Comparison\\_of\\_Qblade\\_and\\_CFD\\_results\\_for\\_small-scaled\\_horizontal\\_axis\\_wind\\_turbine\\_analysis](https://www.researchgate.net/publication/315854164_Comparison_of_Qblade_and_CFD_results_for_small-scaled_horizontal_axis_wind_turbine_analysis) Accessed: 2019-03-20
- [8] Mazur, D.; Trojnar, M. & Smoleń, A. (2011). The Analysis of Wind Turbine with Horizontal Rotation Axis with the Use of Numerical Fluid Mechanics, In: *Analysis and Simulation of Electrical and Computer Systems*, Mazur, Gołębowski & Korkosz (Ed.), 241-249, Springer, 978-3-319-11247-3, New York
- [9] Hosseini, F. & Montekaeef, B. (2017). Innovative Approach to Computer-aided Design of Horizontal Axis Wind Turbine Blades. *Journal of Computation Design and Engineering*, Vol.4, No.2, (April 2017) pp. 98-105, 2288-4300
- [10] Pérez, F. & Trejo, I. (2012). Computer-aided design of horizontal axis turbine blades. *Renewable Energy*, Vol.44, (August 2012) pp. 252-260, 0960-1481
- [11] Gasch, R.; Maurer, J. & Heilmann, C. (2012). Blade Geometry, In: *Wind Power Plants: Fundamentals, Design, Construction and Operation*, Gasch, & Twele (Ed.), 168-203, Springer, 978-3-642-22937-4, New York
- [12] Manwell, J.; McGowan, J. & Rogers, A. (2009). *Wind Energy Explained: Theory, Design and Application*, John Wiley & Sons Ltd., 978-0-470-01500-1, Wiltshire
- [13] Marten, D. & Wendler, J. (2013). QBlade Guidelines v0.6, Available from: <http://q-blade.org/#downloads> Accessed: 2019-03-25
- [14] Ingram, G. (2011). Wind Turbine Blade Analysis Using the Blade Element Momentum Theory, Available from: [https://community.dur.ac.uk/g.l.ingram/download/wind\\_turbine\\_design.pdf](https://community.dur.ac.uk/g.l.ingram/download/wind_turbine_design.pdf) Accessed: 2019-03-26
- [15] (2019) <http://airfoiltools.com> - National Advisory Committee for Aeronautics, SD7062 (14%), Accessed on: 2019-03-29
- [16] Hansen, M. (2008). *Aerodynamics of Wind Turbines*, Earthscan, 978-1-84407-438-9, London
- [17] Schubel, P. & Crossley, R. (2012). Wind Turbine Blade Design. *Energies*, Vol.5, No.9, (September 2012), pp. 3425-3449, 1996-1073
- [18] Marten, D.; Wendler, J.; Pechlivanoglou, G.; Nayeri, C. & Paschereit, C. (2013). QBlade: An Open Source Tool for Design and Simulation of Horizontal and Vertical Axis Wind Turbines. *International Journal of Emerging Technology and Advanced Engineering*, Vol.3, No.3, (February 2013) pp. 264-269, 2250-2459
- [19] Lyon, C.; Broeren, A.; Giguère, P.; Gopalarathnam, A. & Selig, M. (1997). Summary of Low-Speed Airfoil Data, Available from: [https://m-selig.ae.illinois.edu/uiuc\\_lsat/Low-Speed-Airfoil-Data-V3.pdf](https://m-selig.ae.illinois.edu/uiuc_lsat/Low-Speed-Airfoil-Data-V3.pdf) Accessed: 2019-04-05
- [20] Hansen, A. & Butterfield, C. (2003). Aerodynamics of Horizontal-Axis Wind Turbines. *Annual review of fluid mechanics*, Vol.25, No.1, (November 2003) pp. 115-149, 0066-4189
- [21] Celik, A. (2003). Energy Output Estimation for Small-Scale Wind Power Generators Using Weibull-Representative Wind Data. *Journal of Wind Engineering and Industrial Aerodynamics*, Vol.91, No.5, (April 2003) pp. 693-707, 0167-6105
- [22] Sedghi, M.; Hannani, K. & Boroushaki, M. (2015). Estimation of Weibull Parameters for Wind Energy Application in Iran's Cities. *Wind and Structures*, Vol.21, No.2, (August 2015) pp. 203-221, 1226-6116

